

BURN STABILIZATION  
VIA FEEDBACK RIPPLE REGULATION  
IN AN IGNITED TOKAMAK

K. Borrass, M. Söll

IPP 2/262

October 1982



**MAX-PLANCK-INSTITUT FÜR PLASMAPHYSIK**

**8046 GARCHING BEI MÜNCHEN**

**MAX-PLANCK-INSTITUT FÜR PLASMAPHYSIK**  
**GARCHING BEI MÜNCHEN**

BURN STABILIZATION  
VIA FEEDBACK RIPPLE REGULATION  
IN AN IGNITED TOKAMAK

K. Borrass, M. Söll

IPP 2/262

October 1982

*Die nachstehende Arbeit wurde im Rahmen des Vertrages zwischen dem  
Max-Planck-Institut für Plasmaphysik und der Europäischen Atomgemeinschaft über die  
Zusammenarbeit auf dem Gebiete der Plasmaphysik durchgeführt.*

BURN STABILIZATION VIA  
FEEDBACK RIPPLE REGULATION  
IN AN IGNITED TOKAMAK

K. Borrass, M. Söll

October 1982

ABSTRACT

Active burn stabilization of an ignited tokamak by feedback ripple regulation is considered on the basis of recent investigations on ripple-induced transport with insufficient temperature dependence for passive stabilization. Ripple variation is achieved by asymmetric coil currents in the even and odd TF coils. Reference is made to an INTOR-like device. The study comprises a linearized stability analysis based on a O-D plasma description, TF coil calculations relating the current asymmetry to the ripple size and an analysis of the coil/power supply circuitry. Critical performance parameters are obtained in terms of the size of an initial perturbation of the plasma from thermal equilibrium. The performance parameters discussed are the voltages that have to be applied to the TF coils, the powers and energies transferred from external sources and the losses within the TF coils that are associated with the varying field. All critical parameters, subject to technical limitations, are very much on the safe side. The power and energy that have to be transferred from external sources to the TF system can be kept negligibly small by a proper circuit design. No net power is required for the ripple variation. The enhancement of the stationary power requirements by the coil losses is insignificant.

## CONTENTS

1. Introduction
2. Reference System
3. Stability Analysis
4. Magnetic Field Calculations
5. Power Supply Circuit Considerations
6. Alternating Current Losses
7. Conclusion

## 1. INTRODUCTION

Up to now burn control by enhanced ripple losses has been mainly discussed as a passive stabilization method owing to the favourable temperature scaling of the ripple induced loss term in the energy balance. (1, 2, 3) External manipulations are only required in this picture at the beginning of the burn phase, when the ripple has to be raised over its low start-up value. (4, 5) More recent investigations, however, indicate a weaker temperature dependence which no longer suffices for passive stabilization. (6, 7, 8) Feedback control of the field ripple is conceivable as a means of overcoming this difficulty. It is rather obvious and will be demonstrated later in this paper that stabilization is readily possible, provided that the ripple size can be varied with sufficient freedom in amplitude and rate of variation. The main problems arising with this scheme are related to the realization of the required ripple variations and are of a technical nature.

Different methods have been proposed for ripple control, such as asymmetric current variation in different TF coil subsets or the implementation of additional auxiliary coils. (4, 5) In this paper the first method is discussed, specifically the case where there are two subsets, one comprising the odd and one the even numbered TF coils. Because of the extremely high stored energy of a typical ignited tokamak even modest variations of the toroidal field require high energies to be transferred. Since the e-folding time of the instability is of the order of 1 s, the associated powers are also high. High investment costs thus have to be expected for the power supply of the control system. Furthermore the voltages that have to be applied to perform the current variation in the TF coils must not exceed certain limit values in practice. Finally, the alternating TF fields cause different losses within the TF coils which must be kept at an acceptably low value.

To assess the feasibility of the scheme, we evaluate the stated critical quantities for a system which is closely

related to the Phase I version of INTOR. Direct consideration of the Phase I version of INTOR, however, proves inadequate. INTOR, which was designed on the basis of the previous, more pessimistic ripple transport models, has an edge ripple of  $\approx 0.3\%$  (peak to average). The more recent studies require an edge ripple of  $\approx 3\%$  in order to achieve ripple losses comparable with the ALCATOR electron heat conduction losses. As was pointed out in ref. (5), the edge ripple can hardly be increased to this high value in the original INTOR design by asymmetric coil excitation. In order not to hamper our discussion with this artificial drawback yet keep as close as possible to the INTOR discussion, we specify in Sec. 2 a system which is identical to INTOR in its performance objectives but has a higher edge ripple owing to a reduction of the coil number to  $N=8$ .

In Sec. 3 a linear stability analysis is performed in the context of a 0-D plasma model. The formulation is kept rather general and applies to a wide class of ripple loss scalings. Our discussion can thus easily be applied to new findings on ripple transport. As a result the required ripple variation and rate of variation are obtained in terms of an initial temperature perturbation of the system, the gain factor, etc. This yields the input for the next sections.

In Sec. 4 the coil current variation  $\Delta I$  necessary to produce a prescribed ripple variation  $\Delta\delta$  is considered. An analytical expression is derived for the function  $\Delta I(\Delta\delta)$ . The computations are based on the HEDO coil program. (9)

In Sec. 5 the electrical circuit equations for the system comprising the two coil subsets and the respective power supplies are considered. The voltages that must be applied and the powers that have to be delivered from external sources to control a given perturbation of the plasma thermal equilibrium are evaluated.

In Sec. 6 estimates are given for the losses within the TF coils associated with the field variations.

All units are mksa in this paper if not otherwise stated.

## 2. REFERENCE SYSTEM

In this section a reference system meeting the stated requirements on the edge ripple is specified. The calculations were performed with the SUPERCOIL layout model. <sup>(10)</sup> In ref. (10) an example closely reproducing the Phase I version of INTOR was described in greater detail. <sup>(11)</sup> The system to be considered has identical input parameters except that the maximum allowable field ripple at the edge is raised from 0.3 % to 1.5 % and the coil number is reduced to  $N = 8$ . A selective list of parameters for this system is given in Table I. Except for the ripple and the coil number, the main parameters are found to be similar to those of the Phase I version of INTOR. This holds for both plasma and coil data. We emphasize that the specified system is identical to INTOR in its performance objectives and design specifications.

The ripple-induced transport losses should be a small fraction during start-up. The value of 1.24 % meets this requirement in agreement with both refs. (6) and (7).

## 3. STABILITY ANALYSIS

In this section a linear stability analysis of an actively ripple-controlled system is performed in terms of a global plasma description. Apart from its global character and the linearization, the discussion is simplifying in that more subtle effects, such as the shift of the magnetic axis or imperfect confinement of suprathreshold alphas, are ignored. This is adequate for two reasons. Firstly, we are in a situation where continuous progress is made in the understanding of ripple-induced transport and major modifications can be expected. Secondly, the purpose of this paper is the basic assessment of the scheme. In this context an order of magnitude estimate of the ripple variation and speed of variation that are required to bring a system back to equilibrium after it has suffered a realistic perturbation is sufficient. For the same reason we may also confine ourselves to a simple controller.

We consider a pure D-T plasma ( $n = n_e = n_i$ ). Equal temperatures are assumed for ions and electrons ( $T = T_e = T_i$ ). The global energy balance equation then reads

$$3\bar{n}\dot{T} = \bar{Q}_\alpha - \bar{Q}_A - \bar{Q}_R, \quad (1)$$

where it is assumed that  $\bar{n} = \text{const}$  holds as is appropriate in this context.  $\bar{\quad}$  denotes a volume average except for  $\bar{T}$ , which is the density weighted average ( $\bar{T} = \bar{nT}/\bar{n}$ ).  $\bar{Q}_\alpha$  is the  $\alpha$ -heating term. Incomplete confinement of fast  $\alpha$ 's is not taken into account.  $\bar{Q}_A$  describes ALCATOR losses, while  $\bar{Q}_R$  describes the ripple losses. Confinement to ALCATOR-type losses was mainly made to allow a simple comparison with other burn control studies, which mostly rely on this model. ALCATOR-like electron heat conduction losses are assumed to be the dominant transport losses besides ripple losses. Neglecting radiation losses, we assume the system to be transport dominated. This is adequate for a system like INTOR.

A thermal equilibrium point is characterized by the condition (In what follows the average  $\bar{\quad}$  will be omitted for convenience)

$$0 = Q_\alpha^0 - Q_A^0 - Q_R^0. \quad (2)$$

It is convenient to characterize the equilibrium by  $Q_\alpha^0$  and the ratios  $\alpha = Q_A^0/Q_\alpha^0$  and  $\beta = Q_R^0/Q_\alpha^0$ . Equation (2) implies that

$$1 = \alpha + \beta \quad (3)$$

holds.

For  $Q_\alpha$  we assume the scaling

$$Q_\alpha \sim T^2, \quad (4)$$

which is a good approximation in the temperature range of interest. For  $Q_A$  one has

$$Q_A \sim T. \quad (5)$$



For  $Q_R$  we assume the general scaling

$$Q_R \sim T^{f_1} \delta^{f_2}, \quad (6)$$

where  $f_1$  and  $f_2$  are constants to be left open during the general discussion.  $\delta$  always denotes the peak-to-average edge ripple.

Now, assuming all deviations from equilibrium to be of first order, we get from eq. (1) with eqs. (4), (5) and (6) the linearized version of eq. (1) ( $\tilde{\phantom{x}}$  denotes deviations from the equilibrium value, while  $\phantom{x}_0$  denotes equilibrium values;  $T = T_0 + \tilde{T}$  etc.) :

$$\begin{aligned} 3n\dot{\tilde{T}} = & Q_\alpha^0 (1 + 2\tilde{T}/T_0) - \alpha Q_\alpha^0 (1 + \tilde{T}/T_0) \\ & - \beta Q_\alpha^0 (1 + f_1\tilde{T}/T_0 + f_2\tilde{\delta}/\delta_0). \end{aligned} \quad (7)$$

With eq. (3) and the abbreviation  $Q_\alpha^0/3nT_0 = 1/\tau_\alpha$  one gets

$$\dot{\tilde{T}} = \frac{1}{\tau_\alpha} [(2 - \alpha - \beta f_1) \tilde{T} - \beta f_2 T_0 \tilde{\delta}/\delta_0] \quad (8)$$

To get a closed equation for the dynamics of the system, the feedback scheme has to be specified. As a first step we consider the prescription

$$\dot{\tilde{\delta}}_0 = g \frac{\dot{\tilde{T}}}{T_0} \quad (9)$$

together with the initial conditions

$$\tilde{\delta}(0) = 0 \quad \text{and} \quad \tilde{T}(0) = T_1. \quad (10)$$

The gain factor  $g$  is a constant which is yet optional. Equations (9) and (10) prescribe the variation of  $\tilde{\delta}$  in terms of  $\tilde{T}$  in a system with an initially perturbed temperature  $T_0 + T_1$ . This choice for the controller is not unique. It results,

however, in stable solutions and permits a simple formal treatment. Furthermore, such a scheme can easily be realized from a technical point of view, as will be shown later.

From eqs. (9) and (10) we obtain

$$\frac{\partial \tilde{T}}{\partial t} = g \left( \frac{\tilde{T}}{T_0} - \frac{T_1}{T_0} \right) \quad (11)$$

Inserting eq. (11) into eq. (8) yields

$$\dot{\tilde{T}} = \frac{\kappa}{\tau_\alpha} \tilde{T} + \frac{\mu}{\tau_\alpha} T_1, \quad (12)$$

where  $\kappa = 2 - \alpha - \beta f_1 - \beta f_2 g$  and  $\mu = \beta f_2 g$ .

By elementary methods one finds the solution with  $T(0) = T_1$ :

$$\tilde{T} = T_1 \left( e^{\frac{\kappa}{\tau_\alpha} t} - \frac{\mu}{\kappa} + \frac{\mu}{\kappa} e^{\frac{\kappa}{\tau_\alpha} t} \right). \quad (13)$$

Obviously, the system is stable if

$$\kappa = 2 - \alpha - \beta f_1 - \beta f_2 g < 0 \quad (14)$$

holds. In the absence of feedback ( $g = 0$ ) stability requires that

$$f_1 > \frac{2 - \alpha}{\beta} \quad (15)$$

hold, as is well known.

In the stable case the final temperature is given by  $T_0 + \tilde{T}(\infty)$ , where

$$\tilde{T}(\infty) = - T_1 \frac{\mu}{\kappa}. \quad (16)$$

The corresponding total ripple variation that is required to bring the perturbed system back to the ignition curve is given by

$$\frac{\tilde{\delta}(\infty)}{\delta_0} = g \left( \frac{\tilde{T}(\infty)}{T_0} - \frac{T_1}{T_0} \right) = g \frac{T_1}{T_0} \frac{2 - \alpha - \beta f_1}{\alpha + \beta f_1 + \beta f_2 g - 2} \quad (17)$$

$\tilde{\delta}(\infty)/\delta_0$  converges to a lower limit if  $g$  goes to infinity:

$$\frac{\tilde{\delta}(\infty)}{\delta_0} \rightarrow \frac{2 - \alpha - \beta f_1}{\beta f_2} \quad \text{if } g \rightarrow \infty \quad (18)$$

Inserting eq. (13) into eq. (9) gives  $\dot{\delta}$ . In the following section we only need the maximum value of  $\dot{\delta}$  which occurs at  $t = 0$ :

$$\frac{\dot{\delta}_{\max}}{\delta_0} = \frac{g}{\tau_\alpha} \frac{T_1}{T_0} (2 - \alpha - \beta f_1) \quad (19)$$

Finally, we determine the control time. We characterize it by the time  $t_c$  within which the system has performed 1-1/e of the temperature shift when approaching the final state:

$$\begin{aligned} & (e-1) (\tilde{T}(\infty) - T_1)/e \\ & = T_1 \left( e^{\frac{\kappa}{\tau_\alpha} t_c} - \frac{\mu}{\kappa} + \frac{\mu}{\kappa} e^{\frac{\kappa}{\tau_\alpha} t_c} \right) - T_1 \quad (20) \end{aligned}$$

With eq. (16) we get

$$\frac{t_c}{\tau_\alpha} = -\frac{1}{\kappa} = -\frac{1}{2 - \alpha - \beta f_1 - \beta f_2 g} \quad (21)$$

As expected, one has

$$\frac{t_c}{\tau_\alpha} \rightarrow 0 \quad \text{if } g \rightarrow \infty \quad (22)$$

To be more specific, we now consider special figures taking the system specified in Sec. 2. To evaluate  $\tau_\alpha$ , we

estimate  $\bar{\beta}_t$  by  $\bar{\beta}_t = 0.12 \text{ s/A}$  and  $\bar{Q}_\alpha$  by  $\bar{Q}_\alpha = 0.3 \times 10^6 \bar{\beta}_t^2 B_t^{0.4} \text{ Wm}^{-3}$ . (10) With the data of Table I,  $\bar{n} = 1.4 \times 10^{20} \text{ m}^{-3}$  and  $\bar{T} = 10 \text{ keV}$  we then get with the above definition

$$\tau_\alpha \approx 1.2 \text{ s} . \quad (23)$$

Note that our plasma parameters practically coincide with those of the Phase I version of INTOR. (11) INTOR with its underlying transport model is transport dominated and has an ignition margin of roughly 2. Hence, if its layout working point is maintained by additional ripple losses, one must have (approximately)  $\alpha \approx \beta \approx 1/2$ . Following refs. (6), (7), and (8) we assume  $f_1 = 1$  and  $f_2 = 4.5$ , thus assuming to be in a regime where the ripple-induced heat conductivity is virtually temperature independent.

The gain factor  $g$  can, in principle, be chosen freely. In practice, however, it is determined by performance considerations. Firstly, effective control requires that the control time does not exceed the runaway time. On the other hand, the control time should not be smaller than the time for the reorganization of the temperature profile (damping time for profile modes), which is of the order of the energy confinement time. In a transport-dominated system like INTOR the energy confinement time roughly equals the runaway time of the thermal instability. Thus, to meet both requirements, we determine the "optimum" gain factor  $g_0$  by (see eq. (21))

$$\frac{t_c}{\tau_\alpha} = 1 = - \frac{1}{2 - \alpha - \beta f_1 - \beta f_2 g_0} . \quad (24)$$

In our example this yields  $g_0 = 0.889$ .

With these specifications we now get for the reference system

$$\frac{\tilde{\delta}(\infty)}{\delta_0} = 0.889 \frac{T_1}{T_0} , \quad (25)$$

$$\frac{\dot{\delta}_{\max}}{\delta_0} = 0.741 \frac{T}{T_0} \quad (26)$$

and

$$\frac{t_c}{\tau_\alpha} = 1 \quad (27)$$

The quantities  $\tilde{\delta}(\infty)/\delta_0$  and  $\dot{\delta}_{\max}/\delta_0$  represent the required input for the next section.

#### 4. MAGNETIC FIELD CALCULATIONS

In this section the functional dependence is established between the asymmetric current variation and the magnetic field variation at the coils on the one hand and the field ripple on the other hand.

We divide the TF coils into two sets, one comprising the odd and one the even coils. In the following we denote the odd and even coils by the indexes 1 and 2, respectively. The respective conductor currents are  $I_{1/2}$ , while  $\bar{I}_{1/2}$  are the total coil currents. All coils are assumed to be identical except for, possibly, the winding number, which may be  $n_1$  and  $n_2$  for an odd and even coil, respectively. With these definitions

$$\bar{I}_1 = n_1 I_1 \quad (28)$$

and

$$\bar{I}_2 = n_2 I_2 \quad (29)$$

hold.

During plasma start-up all coils have a common total current  $\bar{I}_s$  to minimize the ripple. The corresponding conductor currents  $I_{s1}$  and  $I_{s2}$  are then

$$I_{s1} = \bar{I}_s / n_1 \quad (30)$$

and

$$I_{s2} = \bar{I}_s / n_2 . \quad (31)$$

The total currents  $\bar{I}_1$  and  $\bar{I}_2$  at a later stage are expressed in terms of the initial total current  $\bar{I}_s$  by

$$\bar{I}_1 = \bar{I}_s (1 + X) \quad (32)$$

and

$$\bar{I}_2 = \bar{I}_s (1 + Y) . \quad (33)$$

We impose the constraint that the stored energy of the TF system shall be constant if  $\bar{I}_1$  and  $\bar{I}_2$  vary from their initial value  $\bar{I}_s$ . This then implies that, apart from the losses to be discussed in Sec. 6, no net power is required for the ripple variation. The requirement of constant stored energy establishes a unique relation between Y and X to be derived below. Through this relation the current variation can be characterized by, for instance, X alone.

For the stored energy one easily derives the expression

$$E_m = \frac{1}{2} L_1 I_1^2 + \frac{1}{2} L_2 I_2^2 + L_{12} I_1 I_2 , \quad (34)$$

where

$$L_1 = n_1^2 \bar{L}_1 , \quad (35)$$

$$\bar{L}_1 = \frac{N}{2} \sum_{j=1}^{N/2} \bar{L}_{12j-1} , \quad (36)$$

$$L_2 = n_2^2 \bar{L}_2 , \quad (37)$$

$$\bar{L}_2 = \frac{N}{2} \sum_{j=1}^{N/2} \bar{L}_{22j} , \quad (38)$$

$$L_{12} = n_1 n_2 \bar{L}_{12} \quad (39)$$

and

$$\bar{L}_{12} = \frac{N}{2} \sum_{j=1}^{N/2} \bar{L}_{12j} . \quad (40)$$

Here  $\bar{L}_{ij}$  is the mutual induction between coil  $i$  and  $j$ . The derivation of eqs. (34) to (40) makes use of, besides  $\bar{L}_{ij} = \bar{L}_{ji}$ , the relations  $\bar{L}_{ij} = \bar{L}_i + n_j + n_i$  and  $\bar{L}_{ij} = \bar{L}_i + N_j = \bar{L}_{ij} + N$ . Constancy of  $E_m$  now means that

$$\frac{1}{2} \bar{L}_1 \bar{I}_s^2 (1 + X)^2 + \frac{1}{2} \bar{L}_2 \bar{I}_s^2 (1 + Y)^2 + \bar{L}_{12} \bar{I}_s^2$$

$$(1 + X) (1 + Y) = \frac{1}{2} \bar{L}_1 \bar{I}_s^2 + \frac{1}{2} \bar{L}_2 \bar{I}_s^2 + \bar{L}_{12} \bar{I}_s^2 \quad (41)$$

must hold. Making elementary calculations and using  $\bar{L}_1 = \bar{L}_2$ , one derives from eq. (41) the relation

$$Y = - (1 + k^2 (1 + X))$$

$$+ ((1 + k^2 (1 + X))^2 - X (2 + 2k^2 + X))^{1/2}, \quad (42)$$

which expresses  $Y$  in terms of  $X$ .  $k^2 = \bar{L}_{12}^2 / \bar{L}_1 \bar{L}_2$ . To lowest order in  $X$

$$Y = - X \quad (43)$$

holds as expected.

For the reference system we get with Table II

$$\bar{L}_1 = \bar{L}_2 = 7.7521 \times 10^{-5} \text{ [H]} \quad (44)$$

and

$$\bar{L}_{12} = 4.0113 \times 10^{-5} \text{ [H]} . \quad (45)$$

To establish the functional dependence  $X(\delta)$ , one has to confine oneself to a specific system. Table III summarizes calculations that were performed with the HEDO coil program (9) for the system specified in Sec. 2 . For given coil parameters and coil currents HEDO calculates the magnetic field distribution, the stored energy, the  $\bar{L}_{ij}$  etc.

In a first step HEDO is used to compute the  $\bar{L}_{ij}$  (see Table II). With these  $\bar{L}_{ij}$   $Y$  is then evaluated from  $X$  on the basis of eq. (42) and taken in a second step as input for the HEDO program to compute the field ripple versus  $X$ . In Table III the computed ripple values are given at  $R_0$  (plasma center) and  $R_0 + a$  (boundary). The values for  $E_m$  are added as a check. In addition, the maximum field variation relative to the start-up value ( $X = 0$ ) is added. It typically occurs at the outer coil legs. These data are used in Sec. 6 to estimate the losses within the TF coils.

In the following we only consider the edge ripple. A least square fit by a third-order polynomial was used to approximate the dependence  $X(\delta)$  as contained in Table III:

$$X = - 1.82750 \times 10^{-1} + 1.78681 \times 10^{-1} \delta - 2.78391 \times 10^{-2} \delta^2 + 2.29123 \times 10^{-3} \delta^3 . \quad (46)$$

Here  $\delta$  is in % and eq. (46) applies in the range  $1.24 \% \leq \delta \leq 3.5 \%$ .

Two types of ripple variations have to be distinguished in our discussion. At the end of the heating phase, when



ignition is reached,  $\delta$  has to be raised to some value  $\delta_0$  corresponding to the presumably unstable burn point. We assume that this is also achieved by asymmetric coil excitation corresponding to some value  $X_0$ . Around this equilibrium point small variations  $\tilde{\delta}$  have to be performed to prevent the system from thermal runaway. The corresponding current variations are characterized by  $\tilde{X} = X - X_0$ . The transition to equilibrium is not considered explicitly in this study.

To determine  $\delta_0$ , we rely on refs. (6) and (4). Reference (6) reports transport calculations for an INTOR-like system on the basis of recent ripple loss models. Considering the slight difference in density to the INTOR working point, a value of  $\delta_0 = 3\%$  seems sufficient to result in a 50% contribution (according to  $\alpha = \beta = 0.5$ ) of the ripple losses to the total transport losses. In ref. (4) similar calculations were reported on the basis of previous ripple loss models. Rescaling these results to the recent models also results in a similar value for  $\delta_0$ .

Inserting  $\delta_0$  in eq. (46), we get the equilibrium value of  $X$ :

$$X_0 = 0.16460 \quad . \quad (47)$$

Denoting the equilibrium conductor currents by  $I_{O1}$  and  $I_{O2}$  we have as a consequence of definitions (32) and (33)

$$I_{O1} = I_{S1} (1 + X_0) \quad (48)$$

and

$$I_{O2} = I_{S2} (1 + Y_0) \quad . \quad (49)$$

Since  $\tilde{X}/X_0 \ll 1$  and  $\tilde{\delta}/\delta_0 \ll 1$  are valid, we can conveniently use a linearized version of eq. (46) in the vicinity of the equilibrium point:

$$\tilde{X} = 2.205 \times 10^{-1} \tilde{\delta}/\delta_0 \quad . \quad (50)$$

From eqs. (25), (26) and (50) and the above value for  $X_0$  the following ordering can be verified:

$$\tilde{X} \approx \dot{\tilde{X}} \approx \tilde{Y} \approx \dot{\tilde{Y}} \approx X_0^2 \approx Y_0^2, \quad (51)$$

$$X_0 \ll 1. \quad (52)$$

These relations will be conveniently used in the following section.

### 5. ELECTRICAL CIRCUIT CONSIDERATIONS

In this section we discuss the required power and the voltages that have to be applied in order to perform the ripple variations as specified in Sec. 3. To this end the circuit equations including the two coil subsets have to be discussed. According to the circuit design of Fig. 1 these equations are

$$U_1 = L_1 \dot{I}_1 + L_{12} \dot{I}_2 \quad (53)$$

and

$$U_2 = - (U_1 + U') = L_2 \dot{I}_2 + L_{12} \dot{I}_1 \quad (54)$$

with  $L_1$ ,  $L_2$  and  $L_{12}$  according to eqs. (35), (37) and (39). One advantage of this circuitry is that only the current difference  $I_1 - I_2$  flows through source  $U_1$ . This considerably reduces the powers delivered from sources 1 and 2.

In order to make convenient use of the ordering relations as given by eqs. (51) and (52), we write  $X = X_0 + \tilde{X}$  and  $Y = Y_0 + \tilde{Y}$ , so that

$$I_1 = I_{s1} (1 + X_0 + \tilde{X}) \quad (55)$$

and

$$I_2 = I_{s2} (1 + Y_0 + \tilde{Y}) \quad (56)$$

hold as a consequence of definitions eqs. (30) to (33). For the derivatives we then have

$$\dot{I}_1 = I_{s1} \dot{\tilde{X}} \quad (57)$$

and

$$\dot{I}_2 = I_{s2} \dot{\tilde{Y}} \quad (58)$$

We now consider two different cases as choice of the winding numbers  $n_1$  and  $n_2$  of an odd and even coil, respectively:

CASE 1  $n_1 = n_2 = n$

This means that all coils have the same winding number and are thus completely identical. Hence (see eqs. (30) and (31))

$$I_{s1} = I_{s2} = I_s \quad (59)$$

holds.

For the voltage  $U_1$  we get in this case

$$\begin{aligned} U_1 &= L_1 \dot{I}_1 + L_{12} \dot{I}_2 \\ &= L_1 I_s \dot{\tilde{X}} + L_{12} I_s \dot{\tilde{Y}} \\ &\approx I_s (L_1 - L_{12}) \dot{\tilde{X}} \\ &= \bar{I}_s n (\bar{L}_1 - \bar{L}_{12}) \dot{\tilde{X}} \quad (60) \end{aligned}$$

Here we have used eqs. (59) and (43) and only retained lowest-order contributions.

For the current through source 1 we find with eqs. (59) and (43), retaining only lowest-order terms:

$$\begin{aligned}
 I_1 - I_2 &= I_S (1 + X_O + \tilde{X} - 1 - Y_O - \tilde{Y}) \\
 &\approx 2I_S X_O \\
 &= 2\bar{I}_S X_O / n \quad . \quad (61)
 \end{aligned}$$

For the power delivered by source 1 we now have

$$\begin{aligned}
 P_1 &= U_1 (I_1 - I_2) \\
 &\approx \bar{I}_S^2 (\bar{L}_1 - \bar{L}_{12}) 2X_O \dot{\tilde{X}} \quad . \quad (62)
 \end{aligned}$$

The total energy required to bring the system back to thermal equilibrium after some perturbation at time  $t = 0$  is given by

$$\begin{aligned}
 E(\infty) &= \int_0^\infty dt P_1 \\
 &= \bar{I}_S^2 (\bar{L}_1 - \bar{L}_{12}) 2X_O \tilde{X}(\infty) \quad (63)
 \end{aligned}$$

where  $X(\infty)$  corresponds to  $\tilde{\delta}(\infty)$  according to eq. (50).

With  $\bar{I}_S = 1.85 \times 10^7 \text{A}$ ,  $\bar{L}_1 = 7.752 \times 10^{-5} \text{H}$ ,  $\bar{L}_{12} = 4.011 \times 10^{-5} \text{H}$ ,  $X_O = 0.1646$  and expressing  $\tilde{X}$  by  $\tilde{\delta}/\delta_O$  through eq. (50) we obtain with eqs. (25) and (26) respectively

$$U_1^{\max} = 1.11 \times 10^5 T_1/T_O, \quad (64)$$

$$P_1^{\max} = 6.89 \times 10^8 T_1/T_O \quad (65)$$

and

$$E(\infty) = 8.26 \times 10^8 T_1/T_O \quad . \quad (66)$$

Here  $U_1^{\max}$  and  $P_1^{\max}$  are peak values occurring at  $t = 0$ . For an initial perturbation of  $T_1/T_O = 0.05$  we find for example:

$$U_1^{\max} = 5540 \text{ [V]}, \quad (67)$$

$$P_1^{\max} = 34.4 \text{ [MW]}, \quad (68)$$

$$E(\infty) = 41.3 \text{ [MJ]}. \quad (69)$$

Note that the voltage per coil is only one-fourth of the value given by eqs. (64) and (67).

CASE 2  $I_{O1} = I_{O2}$

Since all coils have a common total current  $\bar{I}_s$  during start-up this implies that the winding numbers of the even and odd coils must be different. From  $I_{s1} = \bar{I}_s/n_1$ ,  $I_{s2} = \bar{I}_s/n_2$  and eqs. (48) and (49) we get

$$\frac{n_1}{n_2} = \frac{1 + X_O}{1 + Y_O} \approx \frac{1 + X_O}{1 - X_O}. \quad (70)$$

For the voltage  $U_1$  we find in this case

$$\begin{aligned} U_1 &= L_1 \dot{I}_1 + L_{12} \dot{I}_2 \\ &= L_1 I_{s1} \dot{\tilde{X}} + L_{12} I_{s2} \dot{\tilde{Y}} \\ &= \bar{I}_s (L_1 \dot{\tilde{X}}/n_1 + L_{12} \dot{\tilde{Y}}/n_2) \\ &= \bar{I}_s n_1 (\bar{L}_1 \dot{\tilde{X}} + \bar{L}_{12} \dot{\tilde{Y}}) \\ &\approx \bar{I}_s n_1 (\bar{L}_1 - \bar{L}_{12}) \dot{\tilde{X}}, \end{aligned} \quad (71)$$

where analogous approximations as in case 1 were performed. In these approximations the voltages  $U_1$  are equal in cases 1 and 2.

For the current that flows through source 1 we find

$$\begin{aligned}
 I_1 - I_2 &= I_{s1} (1 + X_0 + \tilde{X}) - I_{s2} (1 + Y_0 + \tilde{Y}) \\
 &= I_{s1} \tilde{X} - I_{s2} \tilde{Y} \\
 &\approx \bar{I}_s 2\tilde{X}/n_1 \quad , \quad (72)
 \end{aligned}$$

where  $I_{O1} = I_{O2}$  and eq. (70) were used. It is smaller by the ratio  $\tilde{X}/X_0$  than in case 1. Consequently, the power that has to be delivered from the source is also reduced:

$$P_1 = \bar{I}_s^2 (\bar{L}_1 - \bar{L}_{12}) 2\tilde{X}\dot{\tilde{X}} \quad . \quad (73)$$

By integration we get for  $E(\infty)$

$$E(\infty) = \int_0^\infty dt P_1 = \bar{I}_s^2 (\bar{L}_1 - \bar{L}_{12}) \tilde{X}^2(\infty) \quad . \quad (74)$$

By analogy with case 1 one obtains

$$P_1^{\max} = 8.20 \times 10^8 \left( \frac{T_1}{T_0} \right)^2 \quad (75)$$

and

$$E(\infty) = 4.92 \times 10^8 \left( \frac{T_1}{T_0} \right)^2 \quad . \quad (76)$$

For the special perturbation  $T_1/T_0 = 0.05$  this yields

$$P_1^{\max} = 2.05 \quad [\text{MW}] \quad (77)$$

and

$$E(\infty) = 1.23 \quad [\text{MJ}] \quad . \quad (78)$$

These values are an order of magnitude smaller than in case 1.

To benefit fully from the case 2 version, precise knowledge of the equilibrium point is obviously required during the design of the coils. It would thus be most attractive for a reactor which can be built on a definite physical basis and will operate at a fixed burn point. There is, however, a continuous transition from case 1 to case 2 and an increase of  $n_1$  over  $n_2$  may also be advantageous in an experimental device like INTOR.

The control powers we found are quite acceptable and at least do not exceed those for other non-powerless burn control schemes. It is pointed out that this result crucially depends on the circuit design chosen here. Indeed, the power transferred between the two coil sets exceeds the power delivered by external sources by an order of magnitude in case 1 and two orders of magnitude in case 2.

$U' = U_2 - U_1$  is determined in terms of  $U_1$  by the condition of constant stored energy:

$$U' = U_1 (I_1 - I_2)/I_2 \quad . \quad (79)$$

It is obvious that  $I_1 - I_2 / I_2 \ll 1$  is valid in both cases, so that  $U' \ll U_1$  is also true. Hence  $U_1 \approx U_2$  and the restriction on  $U_1$  in the preceding discussion is justified. The values we found for  $U_1$  are considerably below critical values.

We started our discussion in Sec. 3 with a discussion of a desirable plasma dynamics, based on the artificial feedback prescription according to eq. (9) and then determined "backwards" the necessary voltages, that produce the desired ripple variations. Equation (9) can now immediately be transformed into an equivalent prescription for  $U_1$  and  $U_2$ . From eqs. (9), (50) and (60) or (71) we get

$$U_1 \sim \frac{\dot{T}}{T_0} \quad , \quad (80)$$

where the factor of proportionality is determined by  $g$ ,  $X_0$ ,  $\bar{L}_1, \bar{L}_{12}$  etc.  $U'$  is determined by eq. (79). The realization of a controller as defined by eqs. (79) and (80) does not cause any technical problems.

## 6. ALTERNATING CURRENT LOSSES

In this section the losses produced in the TF coils by the alternating toroidal magnetic field are estimated. The toroidal field is directed perpendicularly to the conductor and to the coil casing. Only the AC losses due to variations of "perpendicular magnetic fields" are therefore given.

First the connection between the rate of the magnetic field variation  $\dot{B}$  and the initial temperature perturbation described by  $T_1/T_0$  is established. A least-squares fit by a first-order polynomial is used to approximate the dependence  $\Delta B(X)$  as given by Table III:

$$\Delta B = 2.134 \times 10^{-4} + 5.386X \quad . \quad (81)$$

Note that  $\Delta B$  is the locally maximum field variation, occurring typically at the outer coil legs.

For the rate of the magnetic field variation  $\dot{\tilde{B}}$  one obtains from eq. (81)

$$\dot{\tilde{B}} = 5.386\dot{X} \quad . \quad (82)$$

From eqs. (82), (50) and (26) the maximum value of  $\dot{\tilde{B}}$  in terms of  $T_1/T_0$  is obtained:

$$\dot{\tilde{B}}_{\max} = 0.880 T_1/T_0 \quad . \quad (83)$$

Note that  $\dot{\tilde{B}}_{\max}$  is now the time and local peak rate of the field variations. In what follows we assume that the total TF coil system is exposed to  $\dot{\tilde{B}}_{\max}$ , thus overestimating the AC losses. For a temperature disturbance of  $T_1/T_0 = 0.05$ , for instance, a  $\dot{\tilde{B}}_{\max}$  value of  $4.4 \times 10^{-2} \text{ Ts}^{-1}$  follows.



The AC losses can be subdivided into the hystereses losses, which scale with  $B$ , and the eddy current losses and coupling losses, which scale with  $\dot{B}^2$ .

The hysteresis losses  $P_h$  are given by

$$P_h = \frac{2}{3\pi} V_{sc} j_c \dot{B}, \quad (84)$$

where  $V_{sc}$  is the volume of the superconducting material,  $j_c$  the critical current density of the superconductor, and  $d$  the diameter of the superconducting filaments. For the reference system (see Table I and ref. (10)) eqs. (83) and (84) yield for the hysteresis losses

$$P_h = 2.56 \times 10^4 T_1/T_0. \quad (85)$$

$V_{sc}$  and  $j_c$  were calculated according to the formulas of ref. (10), whereas  $d$  is an input parameter. The values are:  $V_{sc} = 1.6 \text{ m}^3$  ( $\text{Nb}_3\text{S}_n$  as superconductor),  $j_c = 4.3 \times 10^9 \text{ Am}^{-2}$  and  $d = 2. \times 10^{-5} \text{ m}$ . For a special temperature perturbation of  $T_1/T_0 = 0.05$  the value

$$P_h = 1.28 \text{ kW} \quad (86)$$

results.

The eddy current loss terms for conductor and casing and the coupling loss term, which describes the losses produced by induced currents flowing in the conductor core, are collected in one formula:

$$P = \left[ \frac{V_{sc}}{\rho_{e,sc}} \left( \frac{\alpha a^2}{12} + 2 \left( \frac{l_p}{2\pi} \right)^2 \left( 0.5 + \ln \left( \frac{(\alpha + 1)\pi}{8} \right)^{1/2} \right) \right) + \frac{tW^3}{6\rho_{e,ca}} NL \right] \dot{B}^2, \quad (87)$$

where  $\rho_{e,sc}$  and  $\rho_{e,ca}$  are the specific resistivities of the stabilizer and casing,  $a$  is the conductor width and  $l_p$  is the twist length of the filaments. The volume ratio between

stabilizer and superconductor is given by the parameter  $\alpha$ . The eddy current losses produced in the coil casing depend on the thickness  $t$ , the radial width  $W$  of the casing and the circumference  $L$ . The circumference is given by <sup>(10)</sup>

$$L = 2\pi R_1 k e^k [I_0(k) + I_1(k)] \quad (88)$$

where  $k = 1/2 \ln (R_2/R_1)$  and  $R_1, R_2$  are the minimum and maximum distances between the TF centre line and the main torus axis (see, for example, ref. 10). The coupling losses (second term in eq. (87)) are estimated on the assumption that the conductor core, in which the superconducting filaments are embedded, is composed of equal amounts of superconductor and stabilizer. The AC loss formulas are based on ref. 12. With data of the reference system (see Table I and ref. (10)) the losses  $P$  can be expressed by

$$P = 1.60 \times 10^7 (T_1/T_0)^2 \quad (89)$$

$\rho_{e,sc}$ ,  $\alpha$ , and  $W$  are calculated according to ref. (10), while  $W = \Delta + t$  and  $\rho_{e,ca}$ ,  $l_p$  and  $t$  are input data. The data used are:  $\rho_{e,sc} = 4.22 \times 10^{-10} \Omega m$  (including magnetoresistance),  $\rho_{e,ca} = 8.7 \times 10^{-7} \Omega m$ ,  $l_p = 0.1m$ ,  $t = 0.05m$ ,  $\alpha = 116$ ,  $a = 0.016m$  and  $W = 0.98m$ . The width  $a$  is calculated on the assumption that the conductor has an aspect ratio 2 and  $a$  is the smaller length.

For the special perturbation  $T_1/T_0 = 0.05$  eq. (89) yields

$$P = 40.00 \text{ [kW]} \quad (90)$$

This value is an order of magnitude greater than the hysteresis losses.

The total peak losses which have to be cooled away are 41.28 kW. This value has to be considered with respect to the questions whether this can be done without deterioration of the superconducting state and whether the corresponding electrical input power for the refrigerator is kept small enough.

In this study the bath cooling concept is used, with liquid He at a temperature of 4.2K as cooling medium. A maximum temperature increase of the conductor of about 0.5K is allowed, which corresponds to a maximum heat flux of  $\dot{q} = 3 \times 10^3 \text{W/m}^2$ . Assuming a wetting parameter  $\gamma = 0.3 - 0.5$  ( $\gamma$  is the fraction of the conductor which is in direct contact with the coolant), it can be shown that the heat flux produced by the AC losses of 41.28 kW is far below the critical value.

Assuming a refrigerator efficiency of 1/300, an electrical input power for the refrigerator of 12.4 MW results from the AC losses. This amounts to roughly 5 % of the INTOR stationary loads. The electric input power can be further reduced far below 10 MW if conductors with Cu-Ni barriers (high-resistance barriers) are used. In addition the above value is based on a pessimistic estimate of the time and spatial peak values. The actual mean value can be expected to be much lower. The coil losses thus do not significantly enhance the stationary power requirements in an INTOR-like device.

## 7. CONCLUSION

Active burn stabilization of an ignited tokamak via feedback ripple regulation was studied. Recently discovered modifications of the ripple-induced losses, which no longer permit passive stabilization, were taken into account. Only ripple variation by asymmetric excitation of the even and odd TF coils was considered. This scheme does not introduce new design features and preserves as much symmetry of the TF system as possible. Emphasis was placed on discussion of technical aspects of the scheme. Critical parameters under consideration are the voltages at the coils, which must not exceed limit values, and the coil losses, which are due to the varying fields. They must be sufficiently low in order to avoid deterioration of the superconducting state and unacceptable enhancement of the refrigerator power. Finally, the powers and energies that have to be transferred from external power supplies require high investment costs and are thus subject to practical limitations.

From our study the following conclusion can be drawn with respect to the stated critical performance parameters:

1. Voltages of the order of 1 V per turn have to be applied to the TF coils to perform the required ripple variations. They are considerably below critical limits for a typical conductor design.
2. The powers that have to be delivered by external sources are comparable with other non-powerless schemes (compression - decompression, reheating) in the case 1 version. They are even negligibly small in the case 2 version. The same is valid for the transferred energies.
3. Except for the low coil losses no net power from the TF power supply system is required for the ripple variation.
4. Even pessimistic estimates of the coil losses, including eddy current losses in the stabilizer and cryostat, coupling losses and hysteresis losses yield sufficiently low values to avoid local deterioration of the superconducting state.
5. The enhancement of the refrigerator power, caused by the coil losses is insignificant in a system like INTOR.

All critical performance quantities considered are thus very much on the safe side and there is sufficient margin to meet modifications such as may result from further progress on ripple transport or other related fields.

There are some further aspects of the scheme which might be a matter of concern. For instance, the effect of the cyclic load on the coil structure should be estimated. Out-of-plane loads, however, which are particularly undesirable, do not occur at all in our case. This follows for symmetry reasons for our special choice of the coil subsets. In order not to lose this advantage, other possible ways of subdividing the TF coils were ignored.

In our study we have not considered explicitly the problem of how to reach the final working point after having reached ignition at the minimum ripple value  $\delta_s$ . This transition can be understood as a shift of the equilibrium point. In a feedback-controlled system this does not entail any problem, apart from possibly requiring a more refined controller, if this shift is quasistatic, that is, if the transition time is long compared with the control time. As far as the critical performance parameters under consideration are concerned, this case is fully involved in our treatment. Indeed, during the transition phase the system moves into a regime of increasing instability and all critical performance parameters increase monotonously as follows immediately from the preceding discussion. All constraints discussed are thus even better satisfied during the transition phase. A special problem arises, however, for short-burning systems like INTOR, where the length of the transition phase is not necessarily negligibly small compared with the burn time. In this case the necessity of minimizing the duration of the transition phase is given in order to avoid an unfavourable reduction of the duty factor of the system. This problem requires a more refined study and will be treated in a subsequent paper.

REFERENCES

1. T. E. Stringer, Nucl. Fus. Vol. 12 (1972) 689
2. J. W. Connor, R. J. Hastie, Nucl. Fus. Vol. 13 (1973) 221
3. T. W. Petrie, J. M. Rawls, Nucl. Fus. Vol. 20, No. 4 (1980) 419
4. T. W. Petrie, J. M. Rawls, Nucl. Fus. Vol. 20, No. 11 (1980) 1461
5. J. Erb, INTOR Phase II A, European Contributions to the 3rd Workshop Meeting
6. D. E. T. F. Ashby, R. J. Hastie, W. N. G. Hitchon, M. H. Hughes, INTOR Phase II A, European Contributions to the 5th Workshop Meeting, Vol. I, Group A
7. P. N. Yushmanov, Nucl. Fus. Vol. 22, No. 3 (1982) 315
8. K. C. Shaing, J. D. Callen, Nucl. Fus. Vol. 22, No. 8 (1982)
9. P. Martin, H. Preis, Max-Planck-Institut für Plasma-physik Report IPP 3/34 (1977)
10. K. Borrass, M. Söll, Max-Planck-Institut für Plasma-physik Report IPP 4/207 (June 1982)
11. INTOR, International Tokamak Reactor, Phase one, STI/PUB/619 ISBN 92-O-131082-X, IAEA, Vienna (1982)
12. H. Brechna, Superconducting Magnet Systems, Berlin, New York (1973)

a	(m)	1.15	plasma minor radius
A		4.53	plasma aspect ratio
s		1.6	plasma elongation
R <sub>0</sub>	(m)	5.19	plasma major radius
B <sub>t</sub> <sup>0</sup>	(T)	5.70	toroidal field at axis
δ(R)	(%)	1.24	ripple at R = R <sub>0</sub> + a
-----			
R <sub>1</sub>	(m)	2.31	inner coil radius
R <sub>2</sub>	(m)	11.5	outer coil radius
Δ	(m)	0.93	radial thickness of the winding
δ <sub>ins</sub>	(m)	0.15	thermal insulation thickness including the casing thickness
Δ <sub>ax</sub>	(m)	2.18	axial thickness of the winding
I <sub>s</sub>	(A)	1.85 x 10 <sup>7</sup>	total coil current
n		980	number of windings
L <sub>0</sub>	(m)	43.7	average length of a conductor per turn

Table I

Selective list of parameters of the reference system

$\bar{L}_{11}$	(H)	1.5908 x 10 <sup>-5</sup>
$\bar{L}_{12}$	(H)	4.2922 x 10 <sup>-6</sup>
$\bar{L}_{13}$	(H)	1.4575 x 10 <sup>-6</sup>
$\bar{L}_{14}$	(H)	7.2193 x 10 <sup>-7</sup>
$\bar{L}_{15}$	(H)	5.5713 x 10 <sup>-7</sup>

Table II

Inductances for the coil system specified in Sec. 2. The remaining  $\bar{L}_{ij}$  follow from the symmetry relations  $\bar{L}_{ij} = \bar{L}_{ji}$ ,  $\bar{L}_{ij} = \bar{L}_{i+n \ j+n}$  and  $\bar{L}_{ij} = \bar{L}_{i+N \ j} = \bar{L}_{i \ j+N}$

X	0.0	$2.5 \times 10^{-2}$	$5.0 \times 10^{-2}$	$7.5 \times 10^{-2}$	$1.0 \times 10^{-1}$	$1.25 \times 10^{-1}$	$1.5 \times 10^{-1}$	$1.75 \times 10^{-1}$	$2.0 \times 10^{-1}$
$I_1$ (A)	1.85	1.8963	1.9425	1.9888	2.0350	2.0813	2.1275	2.1738	$2.2200 \times 10^7$
Y	0.0	$-2.5200 \times 10^{-2}$	$-5.0808 \times 10^{-2}$	$-7.6833 \times 10^{-2}$	$-1.0329 \times 10^{-1}$	$-1.3018 \times 10^{-1}$	$-1.5753 \times 10^{-1}$	$-1.8535 \times 10^{-1}$	$-2.1365 \times 10^{-1}$
$I_2$ (A)	1.85	1.8034	1.7560	1.7079	1.6589	1.6092	1.5586	1.5071	$1.4548 \times 10^7$
$\delta (R_0)$ (%)	0.21391	0.35821	0.54104	0.76359	1.0191	1.2806	1.54549	1.81326	2.0849
$\delta (a+R_0)$ (%)	1.2379	1.4504	1.6819	1.9316	2.2006	2.4926	2.8046	3.1414	3.5034
$\Delta B$ (T)	0.000	0.135	0.269	0.404	0.539	0.674	0.808	0.943	1.077
$E_m$ (J)	4.0260	4.0260	4.0260	4.0260	4.0260	4.0260	4.0260	4.0260	$4.0260 \times 10^{10}$

Table III

Various HEDO output data versus  $X = \Delta \bar{I}_1 / \bar{I}_s$  for a coil system with data according to Table I



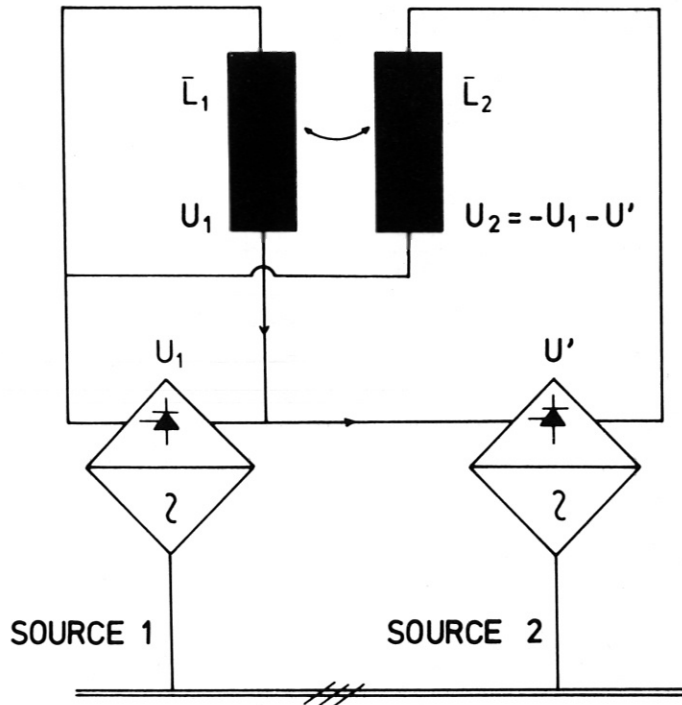


Figure 1

Schematic circuit diagram of the two coil sets and the power supply (The charging phase is not considered.)